*Engineering Transactions,* **70**(1): 53–66, 2022, doi: 10.24423/EngTrans.1720.20220303
Polish Academy of Sciences • Institute of Fundamental Technological Research (IPPT PAN)
Université de Lorraine • Poznan University of Technology

## Research Paper

# Multi-Layered Non-Linear Viscoelastic Beams Subjected to Torsion at a Constant Speed: A Delamination Analysis

Victor Iliev RIZOV[1)*], Holm ALTENBACH[2)]

[1)] *Department of Technical Mechanics*
*University of Architecture, Civil Engineering and Geodesy*
1 Chr. Smirnensky Blvd., 1046 – Sofia, Bulgaria
*Corresponding Author e-mail: v_rizov_fhe@uacg.bg

[2)] *Department of Engineering Mechanics, Institute of Mechanics,*
*Otto-von-Guericke-University*
Magdeburg, Germany
e-mail: holm.altenbach@ovgu.de

A non-linear mechanical model with a linear spring, a linear dashpot and a non-linear dashpot is used for studying the non-linear viscoelastic behaviour of a multi-layered inhomogeneous beam with a delamination crack. The beam with a circular cross-section is under a torsion moment that increases at a constant speed. The non-linear stress-strain-time constitutive law of the model is obtained by adding the non-linear shear strain to the strain in the linear spring and linear dashpot. Solutions of the time-dependent strain energy release rate are derived, which take into account the non-linear viscoelastic behaviour of the beam and the torsion moment rate.

**Key words:** multi-layered beam; non-linear viscoelastic behaviour; delamination.

## 1. Introduction

An efficient alternative to homogeneous materials and structures is the use of continuously inhomogeneous (functionally graded) materials whose properties change in one or more directions [1, 2]. Although the continuously inhomogeneous materials were first applied mainly for thermal protection of space structures, the area of their applicability has quickly expanded due to their superior properties [3–7]. These materials are widely used in various important applications in areas such as aeronautics, nuclear reactors, robotics, mechanical engineering, electronics and biomedicine.

Multi-layered inhomogeneous materials and structural members made of layers of different materials are very useful in lightweight structural applications

due to their high strength-to-weight and stiffness-to-weight ratios [8, 9]. However, since the multi-layered structures have relatively low transversal strength in tension, they are prone to the separation of layers or delamination. Delamination cracks between layers decrease the strength and stiffness of the multi-layered structures. Delamination also reduces the load-bearing ability of structures and affects their reliability and durability. Therefore, delamination analyses of multi-layered structural members pose a problem with a wide practical application.

This paper aims to develop a time-dependent delamination analysis of a multi-layered inhomogeneous beam member with non-linear viscoelastic behaviour. The cross-section of the beam is a circle. The beam is made of concentric longitudinal layers and subjected to a torsion moment at a constant speed. This paper, to some extent, is a continuation of previous publications such as [10, 11]. However, in [10, 11], linear viscoelastic mechanical models representing combinations of linear springs and linear dashpots are applied to describe the viscoelastic behaviour of inhomogeneous beam structures when analysing delamination. In other words, the time-dependent solutions derived in [10, 11] are linear. In reality, however, the mechanical behaviour of viscoelastic materials is usually non-linear, which indicates that the well-known linear viscoelastic models have to be replaced by non-linear ones. Therefore, the most important novelty of this study is that a non-linear viscoelastic mechanical model consisting of a linear dashpot, a linear spring and a non-linear dashpot is used to treat the time-dependent behaviour of the multi-layered inhomogeneous beam. The non-linear constitutive law of the model is derived and then applied to obtain the solution of the strain energy release rate for delamination.

## 2. Delaminated multi-layered non-linear viscoelastic beam under torsion

Consider the non-linear viscoelastic mechanical model shown schematically in Fig. 1. The model consists of a linear spring with the shear modulus $G_i$, mounted in parallel to a linear dashpot with the coefficient of viscosity $\eta_i$. A non-

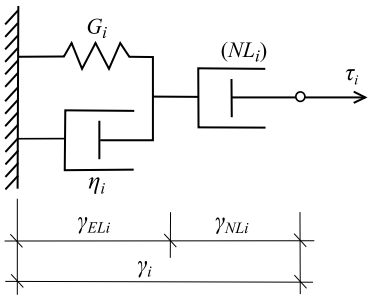


Fig. 1. Mechanical model for the non-linear viscoelastic type of deformation.

linear dashpot $NL_i$ is added to simulate the non-linear viscoelastic behaviour, as shown in Fig. 1. The model is under shear stress $\tau_i$. The variation of $\tau_i$ with time $t$ is expressed as:

$$\tau_i = v_{\tau i} t, \tag{2.1}$$

where $v_{\tau i}$ is the speed.

The model's linear spring and linear dashpot are used for studying the linear viscoelastic shear strain $\gamma_{ELi}$. Thus, the shear strain $\gamma_i$ in the model is written as:

$$\gamma_i = \gamma_{ELi} + \gamma_{NLi}, \tag{2.2}$$

where $\gamma_{NLi}$ is the non-linear viscoelastic shear strain in the non-linear dashpot. The variation of $\gamma_{ELi}$ with time is [12]

$$\gamma_{ELi}(t) = \frac{\tau_i}{t}\mu_i\left(e^{-\lambda_i t} - 1\right) + \frac{\tau_i}{G_i}, \tag{2.3}$$

where

$$\mu_i = \frac{\eta_i}{G_i^2}, \tag{2.4}$$

$$\lambda_i = \frac{G_i}{\eta_i}. \tag{2.5}$$

The shear stress $\tau_{NLi}$, in the non-linear dashpot, is expressed by using the following non-linear relationship [13]:

$$\tau_{NLi} = \alpha_i\left[1 - \left(1 - \frac{\dot{\gamma}_{NLi}}{\beta_i}\right)^{m_i}\right], \tag{2.6}$$

where $\alpha_i$, $\beta_i$, and $m_i$ are material properties, and $\dot{\gamma}_{NLi}$ is the speed of the non-linear shear strain.

Figure 1 indicates that

$$\tau_{NLi} = \tau_i. \tag{2.7}$$

By using Eqs. (2.6) and (2.7), one obtains

$$\dot{\gamma}_{NLi} = \beta_i\left[1 - \left(1 - \frac{\tau_i}{\alpha_i}\right)^{\frac{1}{m_i}}\right]. \tag{2.8}$$

By integrating Eq. (2.8), one derives

$$\gamma_{NLi} = \beta_i t + \frac{\delta_i t}{\tau_i}\left[\left(1 - \frac{\tau_i}{\alpha_i}\right)^{\psi_i} - 1\right], \tag{2.9}$$

where

$$\delta_i = \frac{\alpha_i \beta_i m_i}{1 + m_i}, \tag{2.10}$$

$$\psi_i = \frac{m_i + 1}{m_i}. \tag{2.11}$$

By combining Eqs. (2.2), (2.3), and (2.9), one obtains

$$\gamma_i = \frac{\tau_i}{t}\mu_i \left(e^{-\lambda_i t} - 1\right) + \frac{\tau_i}{G_i} + \beta_i t + \frac{\delta_i t}{\tau_i}\left[\left(1 - \frac{\tau_i}{\alpha_i}\right)^{\psi_i} - 1\right]. \tag{2.12}$$

In fact, relationship (2.12) represents the non-linear constitutive law of the model shown in Fig. 1. This constitutive law is applied to study the non-linear viscoelastic behaviour of the multi-layered beam member shown in Fig. 2.

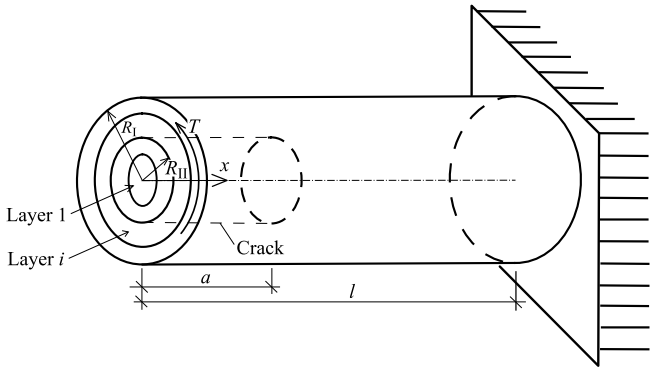


FIG. 2. The multi-layered non-linear viscoelastic beam with a delamination crack under torsion.

The beam under consideration has a circular cross-section of radius $R_{\mathrm{I}}$. The beam consists of an arbitrary number of concentric longitudinal layers, as shown in Fig. 2. Actually, Eq. (2.12) is the constitutive law for the $i$-th layer of the beam. The layers have different thicknesses and material properties. The beam is clamped at its right-hand end. The torsion moment $T$, applied at the beam free end, varies with time according to the following dependence:

$$T = vt, \tag{2.13}$$

where $v$ is the speed.

The length of the beam is denoted by $l$. A delamination crack of length $a$ is located in the beam, as shown in Fig. 2. The delamination is a circular cylindrical surface of the radius $R_{\mathrm{II}}$. Therefore, the inner crack arm has a circular cross-section with the radius $R_{\mathrm{II}}$. The cross-section of the outer crack arm is a ring

with internal and external radiuses $R_{\mathrm{II}}$ and $R_{\mathrm{I}}$, respectively. The inner crack arm is free of stresses. The beam layers are continuously inhomogeneous in the longitudinal direction. Therefore, the material properties involved in the constitutive law (2.12) vary continuously along the beam length. The variation of material properties in the $i$-th layer is presented as:

$$\alpha_i = \alpha_{kpi} + \frac{\alpha_{bpi} - \alpha_{kpi}}{l^{\varphi_{\alpha i}}} x^{\phi_{\alpha i}}, \tag{2.14}$$

$$\beta_i = \beta_{kpi} + \frac{\beta_{bpi} - \beta_{kpi}}{l^{\varphi_{\beta i}}} x^{\phi_{\beta i}}, \tag{2.15}$$

$$m_i = m_{kpi} + \frac{m_{bpi} - m_{kpi}}{l^{\varphi_{mi}}} x^{\phi_{mi}}, \tag{2.16}$$

$$\eta_i = \eta_{kpi} + \frac{\eta_{bpi} - \eta_{kpi}}{l^{\varphi_{\eta i}}} x^{\phi_{\eta i}}, \tag{2.17}$$

$$G_i = G_{kpi} + \frac{G_{bpi} - G_{kpi}}{l^{\varphi_{Gi}}} x^{\phi_{Gi}}, \tag{2.18}$$

where

$$0 \leq x \leq l, \tag{2.19}$$

$$i = 1, 2, ..., n. \tag{2.20}$$

In Eqs. (2.14)–(2.20), $n$ is the number of beam layers, $x$ is the longitudinal centroidal axis of the beam, $\alpha_{kpi}$, $\beta_{kpi}$, $m_{kpi}$, $\eta_{kpi}$, and $G_{kpi}$ are the values of $\alpha_i$, $\beta_i$, $m_i$, $\eta_i$, and $G_i$ at the free end of the beam, respectively. The values of $\alpha_i$, $\beta_i$, $m_i$, $\eta_i$, and $G_i$ at the clamped end of the beam are denoted by $\alpha_{bpi}$, $\beta_{bpi}$, $m_{bpi}$, $\eta_{bpi}$, and $G_{bpi}$, respectively. The parameters $\phi_{\alpha i}$, $\phi_{\beta i}$, $\phi_{mi}$, $\phi_{\eta i}$, and $\phi_{Gi}$ control the material inhomogeneity along the length of the layer.

The purpose of the present analysis is to derive a solution of the strain energy release rate $G$ for the delamination in the beam in Fig. 2, which takes into account the non-linear viscoelastic behaviour. The strain energy release rate is obtained as:

$$G = \frac{\mathrm{d}U^*}{\mathrm{d}A}, \tag{2.21}$$

where $U^*$ is the complementary strain energy in the beam, and $\mathrm{d}A$ is an elementary increase of the delamination crack area. Formula (2.21) is re-written as:

$$G = \frac{\mathrm{d}U^*}{2\pi R_{\mathrm{II}}\,\mathrm{d}a}, \tag{2.22}$$

since

$$\mathrm{d}A = 2\pi R_{\mathrm{II}}\,\mathrm{d}a, \tag{2.23}$$

where $\mathrm{d}a$ is an elementary increase of the delamination crack length.

The complementary strain energy is written as:

$$U^* = U^*_{cr} + U^*_{uc}, \tag{2.24}$$

where $U^*_{cr}$ and $U^*_{uc}$ are complementary strain energies in the outer crack arm and in the un-cracked beam portion $a \leq x \leq l$, respectively.

The quantity $U^*_{cr}$ is obtained by integrating the complementary strain energy density in the volume of the outer crack arm as follows:

$$U^*_{cr} = \sum_{i=1}^{i=n_1} \int_0^a \int_{R_i}^{R_{i+1}} u^*_{0i} 2\pi R\,\mathrm{d}R\,\mathrm{d}x, \tag{2.25}$$

where $n_1$ is the number of layers in the outer crack arm, $R_i$ and $R_{i+1}$ are the internal and external radiuses of the $i$-th concentric layer, $u^*_{0i}$ is the complementary strain energy density in the layer, and $R$ is a running radius.

Since strain is expressed as a non-linear function of stress (refer to the constitutive law (2.12)), the complementary strain energy density is written as:

$$u^*_{0i} = \int_0^{\tau_i} \gamma_i(\tau_i)\,\mathrm{d}\tau_i. \tag{2.26}$$

By combining Eqs. (2.12) and (2.26), one derives

$$u^*_{0i} = \frac{\tau_i^2 \mu_i}{2t}\left(e^{-\lambda_i t} - 1\right) + \frac{\tau_i^2}{2G_i} + \beta_i \tau_i t - \delta_i t + \frac{\alpha_i \delta_i t}{2\tau_i}\left[1 - \left(1 - \frac{\tau_i}{\alpha_i}\right)^2\right]. \tag{2.27}$$

Due to the non-linear character of the constitutive law (2.12), the stress cannot be determined explicitly from Eq. (2.12). Therefore, the expression of the complementary strain energy (2.25) is re-written as:

$$U^*_{cr} = \sum_{i=1}^{i=n_1} \int_0^a \int_{\tau_{dli}}^{\tau_{gri}} u^*_{0i} 2\pi R\,\mathrm{d}R\,\mathrm{d}x, \tag{2.28}$$

where $\tau_{dli}$ and $\tau_{gri}$ are the shear stresses at the internal and external surfaces of the $i$-th layer of the beam.

The quantities $R$ and $\mathrm{d}R$ in Eq. (2.28) are expressed as functions of $\tau_i$ in the following way. First, the distribution of the shear strains in the cross-section of the outer crack arm is found as:

$$\gamma = \frac{\gamma_\zeta}{R_{\mathrm{I}}} R, \tag{2.29}$$

where

$$R_{\mathrm{II}} \leq R \leq R_{\mathrm{I}}. \tag{2.30}$$

In Eq. (2.29), $\gamma_\zeta$ is the shear stress at the surface of the beam. Distribution (2.29) follows from the fact that the validity of the Bernoulli's hypothesis for plane sections is assumed here since beams of high length-to-diameter ratio are under consideration. By using Eq. (2.29), one obtains

$$R = \frac{\gamma}{\gamma_\zeta} R_{\mathrm{I}}. \tag{2.31}$$

By combining Eqs. (2.12) and (2.31), one derives

$$R = \frac{R_I}{\lambda_\zeta} \left\{ \frac{\tau_i}{t} \mu_i \left( e^{-\lambda_i t} - 1 \right) + \frac{\tau_i}{G_i} + \beta_i t + \frac{\delta_i t}{\tau_i} \left[ \left( 1 - \frac{\tau_i}{\alpha_i} \right)^{\psi_i} - 1 \right] \right\}. \tag{2.32}$$

From Eq. (2.32), one obtains

$$\begin{aligned} \mathrm{d}R = \frac{R_{\mathrm{I}}}{\lambda_\zeta} \Bigg\{ & \frac{1}{t} \mu_i \left( e^{-\lambda_i t} - 1 \right) + \frac{1}{G_i} \\ & + \delta_i t \left\{ -\frac{1}{\tau_i^2} \left[ \left( 1 - \frac{\tau_i}{\alpha_i} \right)^{\psi_i} - 1 \right] - \frac{1}{\tau_i} \psi_i \left( 1 - \frac{\tau_i}{\alpha_i} \right)^{\psi_i - 1} \frac{1}{\alpha_i} \right\} \Bigg\} \mathrm{d}\tau_i. \end{aligned} \tag{2.33}$$

The shear stresses at the internal and external surfaces of the beam layers, which are involved in Eq. (2.25), are found by using the following equations:

$$\frac{\gamma_\zeta}{R_{\mathrm{I}}} R_i = \frac{\tau_{dli}}{t} \mu_i \left( e^{-\lambda_i t} - 1 \right) + \frac{\tau_{dli}}{G_i} + \beta_i t + \frac{\delta_i t}{\tau_{dli}} \left[ \left( 1 - \frac{\tau_{dli}}{\alpha_i} \right)^{\psi_i} - 1 \right], \tag{2.34}$$

$$\frac{\gamma_\zeta}{R_I} R_{i+1} = \frac{\tau_{gri}}{t} \mu_i \left( e^{-\lambda_i t} - 1 \right) + \frac{\tau_{gri}}{G_i} + \beta_i t + \frac{\delta_i t}{\tau_{gri}} \left[ \left( 1 - \frac{\tau_{gri}}{\alpha_i} \right)^{\psi_i} - 1 \right], \tag{2.35}$$

where $i = 1, 2, ..., n_1$.

It should be mentioned that Eqs. (2.34) and (2.35) are obtained by combining Eqs. (2.12) and (2.29). One additional equation is written by considering the equilibrium of the elementary forces in the outer crack arm:

$$T = \sum_{i=1}^{i=n_1} \int_{\tau_{dli}}^{\tau_{gri}} \tau_i 2\pi R^2 \, \mathrm{d}R, \tag{2.36}$$

where $R$ and $\mathrm{d}R$ are found by Eqs. (2.32) and (2.33). There are $2n_1 + 1$ unknowns, $\tau_{dli}$, $\tau_{gri}$, and $\gamma_\zeta$, where $i = 1, 2, ..., n_1$ in (2.34)–(2.36). The MatLab computer program is used to solve Eqs. (2.34)–(2.36) with respect to $\tau_{dli}$, $\tau_{gri}$, and $\gamma_\zeta$ at various values of time.

Equation (2.28) is also used to determine the complementary strain energy in the un-cracked beam portion. For this purpose, $n_1$ and $u^*_{0i}$ are replaced with $n$ and $u^*_{0uci}$ where $u^*_{0uci}$ is the complementary strain energy density in the $i$-th layer of the un-cracked portion of the beam. Also, $n_1$ is replaced with $n$ in Eqs. (2.34) and (2.36).

By combining Eqs. (2.22), (2.24), and (2.28), one derives

$$G = \frac{1}{2\pi R_{\mathrm{II}}} \left( \sum_{i=1}^{i=n_1} \int_{\tau_{dli}}^{\tau_{gri}} u^*_{0uni} 2\pi R \, \mathrm{d}R - \sum_{i=1}^{i=n} \int_{\tau_{dli}}^{\tau_{gri}} u^*_{0uni} 2\pi R \, \mathrm{d}R \right), \tag{2.37}$$

where the complementary strain energy densities are obtained at $x = a$. Integration in (2.37) is performed by the MatLab computer program. Formula (2.37) is applied to calculate the strain energy release rate at various time values.

The strain energy release rate is also derived by analysing the balance of the energy. For this purpose, the following equation is used:

$$T\delta\phi = \frac{\partial U}{\partial a}\delta a + G l_{cf} \delta a, \tag{2.38}$$

where $\phi$ is the angle of twist of the free end of the outer crack arm, $U$ is the strain energy in the beam, $l_{cf}$ is the length of the crack front, and $\delta a$ is a small increase of the crack length. The quantity $l_{cf}$ is written as:

$$l_{cf} = 2\pi R_{\mathrm{II}}. \tag{2.39}$$

By using Eqs. (2.38) and (2.39), one obtains

$$G = \frac{1}{2\pi r_1} \left( T \frac{\partial \phi}{\partial a} - \frac{\partial U}{\partial a} \right). \tag{2.40}$$

The strain energy is found by Eqs. (2.24) and (2.28). For this purpose, the complementary strain energy density is replaced with the strain energy density $u_{0i}$, which is written as:

$$u_{0i} = \tau_i \gamma_i - u_{0i}^*, \tag{2.41}$$

where $\gamma_i$ and $u_{0i}^*$ are expressed by (2.12) and (2.27), respectively.

The integrals of Maxwell-Mohr find the angle of twist involved in Eq. (2.40):

$$\phi = \int_0^a \frac{\gamma_\zeta}{R_i}\,\mathrm{d}x + \int_a^l \frac{\gamma_\xi}{R_I}\,\mathrm{d}x, \tag{2.42}$$

where $\gamma_\xi$ is the shear strain at the surface of the un-cracked portion of the beam.

By combining Eqs. (2.24), (2.28), (2.40), and (2.42), one derives

$$G = \frac{1}{2\pi R_1}\left[T\left(\frac{\gamma_\zeta}{R_1} - \frac{\gamma_\xi}{R_2}\right) - \sum_{i=1}^{i=n_1}\int_{\tau_{dli}}^{\tau_{gri}} u_{0i} 2\pi R\,\mathrm{d}R + \sum_{i=1}^{i=n}\int_{\tau_{dli}}^{\tau_{gri}} u_{0uni} 2\pi R\,\mathrm{d}R\right]. \tag{2.43}$$

The quantities involved in Eq. (2.43) are obtained at $x = a$. The integration is carried-out by the MatLab computer program. Calculations of the strain energy release rate are performed at various time values. The strain energy release rates found by Eq. (2.43) are exact matches of the ones obtained by using Eq. (2.37), which confirms the correctness of the solutions.

It should be specified that the strain energy release rate derived here is time-dependent since the material has viscoelastic behaviour and the beam is under time-dependent torsion moment.

## 3. Numerical results

The numerical results presented here are obtained using the strain energy release rate solution derived in Sec. 2 of this paper. The strain energy release rate is written in non-dimensional form by applying the formula $G_N = G/\left(G_{kp1} R_\mathrm{I}\right)$. Two three-layered non-linear viscoelastic cantilever beam configurations under torsion are considered (the only difference between these configurations is the location of the delamination crack). In the first beam configuration, delamination is located between layers 1 and 2. In the second beam configuration, delamination is between layers 2 and 3. It is assumed that $l = 0.400$ m, $R_\mathrm{I} = 0.010$ m and $v = 0.8 \cdot 10^{-8}$ N$\cdot$m/s.

The variation of the strain energy release rate with time is analysed by performing calculations of the strain energy release rate at various time values. The beam configuration with a delamination crack located between layers 2 and 3 is considered. Figure 3 shows the strain energy release rate variation

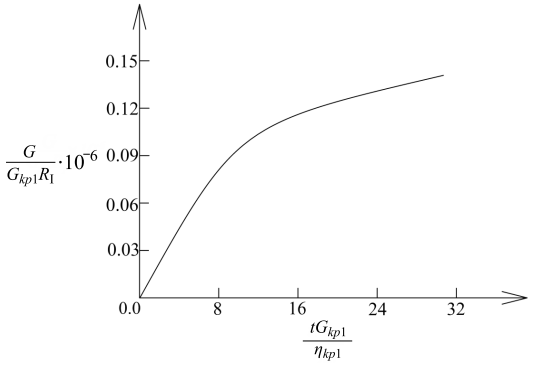


FIG. 3. Variations of the strain energy release rate with time.

with time (the latter is expressed in non-dimensional form by formula $t_N = tG_{kp1}/\eta_{kp1}$). It can be observed that the strain energy release rate increases with time (Fig. 3).

The effect of the continuous variation of $\alpha_1$ along the beam length in layer 1 is also analysed. Both beam configurations (delamination between layers 1 and 2 and delamination between layers 2 and 3) are considered. The corresponding results are shown in Fig. 4, where the strain energy release rate is plotted against $\alpha_{bp1}/\alpha_{kp1}$ ratio (this ratio characterizes the variation of $\alpha_1$). In Fig. 4, one can observe that the strain energy release rate decreases with increasing of $\alpha_{bp1}/\alpha_{kp1}$ ratio. Figure 4 also indicates that the strain energy release rate in the beam configuration with delamination crack located between layers 2 and 3 is higher than that in the configuration with delamination between layers 1 and 2. This finding is attributed to the fact that when delamination is between layers 2 and 3 the stiffness of the outer crack arm is lower compared to the case when delamination is located between layers 1 and 2.

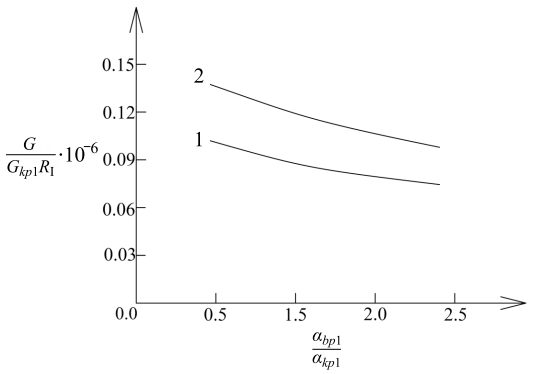


FIG. 4. Variations of the strain energy release rate with $\alpha_{bp1}/\alpha_{kp1}$ ratio (curve 1 – for the three-layered beam with delamination between layers 1 and 2, curve 2 – for the three-layered beam with delamination between layers 2 and 3).

Figure 5 depicts the strain energy release rate variation with $\eta_{bp1}/\eta_{kp1}$ ratio at three $a/l$ ratios. It should be mentioned that $\eta_{bp1}/\eta_{kp1}$ and $a/l$ ratios characterize the variation of $\eta_1$ in layer 1 along the beam length and the relative beam length, respectively. The curves in Fig. 5 indicate that the strain energy release rate decreases with increasing of $\eta_{bp1}/\eta_{kp1}$ ratio. An increase of $a/l$ ratio also leads to a decrease of the strain energy release rate (Fig. 5).

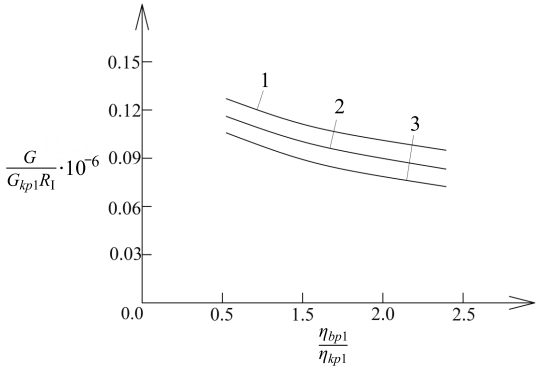


FIG. 5. Variations of the strain energy release rate with $\eta_{bp1}/\eta_{kp1}$ ratio (curve 1 – at $a/l = 0.3$, curve 2 – at $a/l = 0.5$, curve 3 – at $a/l = 0.7$).

The variation of the strain energy release rate with $\eta_{kp2}/\eta_{kp1}$ and $\eta_{kp3}/\eta_{kp1}$ ratios is illustrated in Fig. 6. In Fig. 6, it is observed that the strain energy release rate decreases with increasing of $\eta_{kp2}/\eta_{kp1}$ and $\eta_{kp3}/\eta_{kp1}$ ratios.

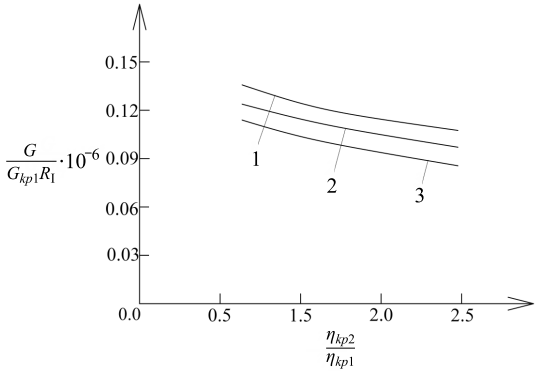


FIG. 6. Variations of the strain energy release rate with $\eta_{kp2}/\eta_{kp1}$ ratio (curve 1 – at $\eta_{kp3}/\eta_{kp1} = 0.5$, curve 2 – at $\eta_{kp3}/\eta_{kp1} = 1.5$, curve 3 – at $\eta_{kp3}/\eta_{kp1} = 2.5$).

The effect of the continuous variation of the shear modulus $G_1$ along the beam length in layer 1 on the strain energy release rate is shown in Fig. 7, where the strain energy release rate is plotted against $G_{bp1}/G_{kp1}$ ratio at three speeds of torsion moment $v$. In Fig. 7, it can be observed that the strain energy

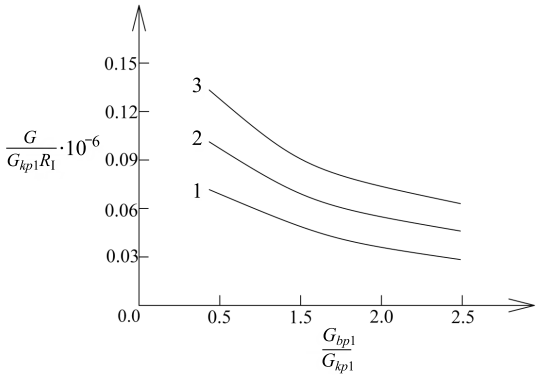


FIG. 7. Variations of the strain energy release rate with $G_{bp1}/G_{kp1}$ ratio (curve 1 – at $v = 0.3 \cdot 10^{-8}$ N · m/s, curve 2 – at $v = 0.6 \cdot 10^{-8}$ N · m/s, curve 3 – at $v = 0.8 \cdot 10^{-8}$ N · m/s).

release rate decreases with increasing $G_{bp1}/G_{kp1}$ ratio. The increase of the speed $v$ leads to an increase of the strain energy release rate (Fig. 7).

Finally, the strain energy release rate is obtained assuming the linear viscoelastic behaviour of the beam member. For this purpose, $\beta_i = 1$ and $m_i = 1$ are substituted in the non-linear solution derived in Sec. 2 of this paper. This follows from the fact that at $\beta_i = 1$ and $m_i = 1$ the non-linear relationship (2.6) transforms into $\tau_{NLi} = \alpha_i \dot{\gamma}_{NLi}$, which represents the constitutive law of a linear dashpot with the coefficient of viscosity $\alpha_i$, and, in this way, the non-linear model depicted in Fig. 1 transforms into the linear viscoelastic model with a linear spring and two linear dashpots. The strain energy release rate derived using both non-linear and linear solutions is plotted against $G_{kp2}/G_{kp1}$ ratio in Fig. 8. In Fig. 8, the curves show that the strain energy release rate increases when non-linear viscoelastic behaviour is assumed. Also, one can observe that the strain energy release rate decreases with increasing of $G_{kp2}/G_{kp1}$ ratio.

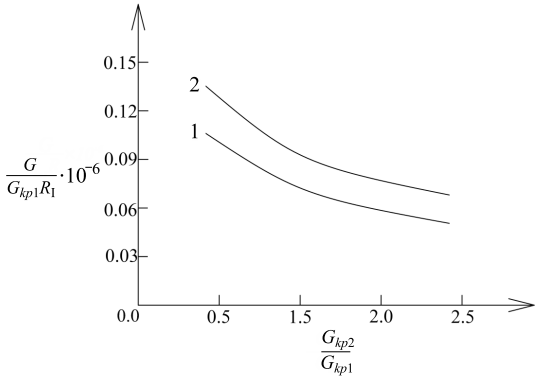


FIG. 8. Variations of the strain energy release rate with $G_{kp2}/G_{kp1}$ ratio (curve 1 – at linear viscoelastic behaviour, curve 2 – at non-linear viscoelastic behaviour).

## 4. Conclusion

A non-linear dashpot was added to a mechanical model consisting of a linear spring mounted parallel to a linear dashpot in order to simulate the non-linear viscoelastic behaviour of a multi-layered inhomogeneous cantilever beam member of circular cross-section with a delamination crack. The beam was under a torsion moment that increased at a constant speed. The non-linear dashpot in the model obeyed a non-linear relationship between the shear stress and the rate of the shear strain. The shear strain in the non-linear dashpot was obtained by integrating the non-linear stress-strain relationship. The stress-strain-time constitutive law of the model was found by adding the strain in the non-linear dashpot to the strain in the linear spring and linear dashpot. The beam layers are continuously inhomogeneous along the beam length. Therefore, the material properties involved in the constitutive law of the model vary continuously in the longitudinal direction. This constitutive law was applied to model the time-dependent non-linear viscoelastic behaviour when deriving a solution of the strain energy release rate for the delamination crack. Since the beam displayed non-linear viscoelastic behaviour, the strain energy release rate was found by considering the complementary strain energy. The solution obtained is time-dependent and takes into account the non-linear viscoelastic behaviour and the torsion moment speed. A time-dependent non-linear solution of the strain energy release rate was also derived by analysing the balance of the energy with considering the non-linear viscoelastic behaviour for verification. The variation of the strain energy release rate with time was analysed. It is found that the strain energy release rate increases with time. The effect of material inhomogeneity of the layers in the longitudinal direction on the strain energy release rate was evaluated. It was ascertained that the strain energy release rate decreases with increasing of $\alpha_{bp1}/\alpha_{kp1}$, $\eta_{bp1}/\eta_{kp1}$, $\eta_{kp2}/\eta_{kp1}$, $\eta_{kp3}/\eta_{kp1}$, $G_{bp1}/G_{kp1}$, and $G_{kp2}/G_{kp1}$ ratios. The increase of the speed of the torsion moment also led to an increase of the strain energy release rate. The strain energy release rate was also derived for the case of linear viscoelastic behaviour of the beam. It was found that the non-linear viscoelastic behaviour leads to an increase of the strain energy release rate.

## Acknowledgments

V.I. Rizov gratefully acknowledges the German Academic Exchange Organization (DAAD) for the financial support of his research conducted during his stay at the Department of Engineering Mechanics, Institute of Mechanics, Otto-von-Guericke-University, Magdeburg, Germany.

## References


1. Bohidar S.K., Sharma R., Mishra P.R., Functionally graded materials: A critical review, *International Journal of Research*, **1**(7): 289–301, 2014.
2. Mahamood R.M., Akinlabi E.T., *Functionally Graded Materials*, Springer International Publishing, 2017, doi: 10.1007/978-3-319-53756-6.
3. Çallioğlu H., Sayer M., Demir E., Stress analysis of functionally graded discs under mechanical and thermal loads, *Indian Journal of Engineering and Materials Sciences*, **18**(2): 111–118, 2011.
4. Çallioğlu H., Sayer M., Demir E., Elastic-plastic stress analysis of rotating functionally graded discs, *Thin-Walled Structures*, **94**: 38–44, 2015, doi: 10.1016/j.tws.2015.03.016.
5. Demir E., Çallioglu H., Sayer M., Free vibration of symmetric FG sandwich Timoshenko beam with simply supported edges, *Indian Journal of Engineering and Materials Sciences*, **20**(6): 515–521, 2013, http://nopr.niscair.res.in/handle/123456789/25586.
6. Akbulut M., Sonmez F.O., Optimum design of composite laminates for minimum thickness, *Computers & Structures*, **86**(21–22): 1974–1982, 2008, doi: 10.1016/j.compstruc.2008.05.003.
7. Akbulut M., Sarac A., Ertas A.H., An investigation of non-linear optimization methods on composite structures under vibration and buckling loads, *Advances in Computational Design*, **5**(3): 209–231, 2020, doi: 10.12989/acd.2020.5.3.209.
8. Nguyen S.-N., Lee J., Han J.-W., Cho M., A coupled hygrothermo-mechanical viscoelastic analysis of multilayered composite plates for long-term creep behaviors, *Composite Structures*, **242**: 112030, 2020, doi: 10.1016/j.compstruct.2020.112030.
9. Nguyen S.-N., Lee J., Cho M., Application of the Laplace transformation for the analysis of viscoelastic composite laminates based on equivalent single-layer theories, *International Journal of Aeronautical and Space Sciences*, **13**(4): 458–467, 2012, doi: 10.5139/ijass.2012.13.4.458.
10. Rizov V.I., Analysis of two lengthwise cracks in a viscoelastic inhomogeneous beam structure, *Engineering Transactions*, **68**(4): 397–415, 2020, doi: 10.24423/EngTrans.1214.20201125.
11. Rizov V.I., Longitudinal vertical crack analysis in beam with relaxation stresses, *World Journal of Engineering*, **18**(3): 452–457, 2020, doi: 10.1108/WJE-05-2020-0181.
12. Zubchaninov V.G., *Fundamentals of Theory of Elasticity and Plasticity*, Moscow: Vishaya Shkola Press, 1990.
13. Lukash P.A., *Fundamentals of Non-linear Structural Mechanics* [in Russian], Moscow: Stroiizdat, 1978.


*Received December 10, 2021; accepted version January 14, 2022.*